Development and Testing of a Thermal Battery Utilizing Concrete and Thermosiphons for Power Plant Flexibilization

Conference Paper · August 2022

16 authors, including:

Julio Bravo
Lehigh University

Ahmed Abdulridha
Lehigh University

Shuoyu Wang
Lehigh University

Development and Testing of a Thermal Battery Utilizing Concrete and Thermosiphons for Power Plant Flexibilization

Julio Bravo [a], Ahmed Abdulridha [b], Shuoyu Wang [b], Justin Caspar [a], Dominic Matrone [a], Hans Agarwal [a], Zheng Yao [a], Sudhakar Neti [a], Alparslan Oztekin [a], Clay Naito [b], Spencer Quiel [b], Muhannad Suleiman [b], Yue Xiao [c], Devon Jensen [c], Chien-Hua Chen [c], Carlos Romero [a,*]

[a] Energy Research Center, Lehigh University, 117 ATLSS Drive, Bethlehem, PA 18015, USA
[b] ATLSS Engineering Research Center, Lehigh University, 117 ATLSS Drive, Bethlehem, PA 18015, USA
[c] Advanced Cooling Technology, Inc., 1046 New Holland Ave Building 2, Lancaster, PA 17601

Abstract

A fast increase in power generation from renewable sources is creating the need for a larger contribution from power generation from other sources. This demands more flexible power generation systems, making energy storage a necessity to integrate flexible power generation with the grid demand. Thermal energy storage is a good option to be integrated with Rankine power cycles. Particularly, sensible heat stored in concrete offers the option for integration with power plants in a flexible and cost competitive way. This paper reports research results performed by Lehigh University for the development of a thermal battery cell (TBC) capable of operating at temperatures up to 450°C. The Lehigh TBC integrates a concrete matrix, engineered to provide enhanced thermal and mechanical properties, and thermosiphon elements capable of dual action operation, engineered to enable charging and discharging on a single thermal battery unit. Components for the TBC were researched in the laboratory, and an integrated single-thermosiphon, 10 kWh_{th} TBC was designed and tested. Efficient heat transfer to/from the storage media, was demonstrated in the lab. The 10 kWh_{th} TBC was tested under several different charging and discharging conditions and proven to be resourceful. Test results demonstrate the feasibility of the concept to store sensible thermal energy in concrete between 300°C and 400°C, with fast charging and discharging performance provided by the thermosiphon, suited for fast ramping of the power generation unit. The Lehigh University team is working on the design, construction and testing of a scale-up 100-kWh_{th} TBC prototype which will integrate multiple optimized thermosiphons, a constrained concrete formulation, and computationally optimized charge/discharge plenums.

1. Introduction

The need to reduce carbon dioxide (CO_2) emissions to mitigate the impact of greenhouse gases on the severity of global climate change has promoted an increase in the use of energy from renewable sources. The contribution of energy from renewable sources has increased on the grid, creating a scenario where fossil fired power plants are faced, with the necessity to operate at conditions different than their intended design, such as cycling and operating below minimum low-load design condition. These new grid conditions have forced fossil fuel fired power plants to become flexible, in order to adapt to new electrical system operator market opportunities.

Since power generation from renewables has not raised yet to satisfy the grid demand, fossil fuel fired power plants need to continue being operated during the transition to a carbon-constrained future. To allow a smooth transition, research on fossil fuel fired power plants flexibilization has become very active. The use of thermal energy storage integrated with fossil fuel fired power plants is one of the options for power plants flexibilization. (Cao et al., 2020) integrated a high-temperature energy storage-aided cycle into the steam-water cycle of a conventional coal power plant to assess the round-trip efficiency of the integrated concept. (Richter et al., 2015) modeled and validated a detailed non-steady coal fired power plant steam generator in Modelica/Dymola using the library Clara (Clausius-Rankine) and demonstrated an efficient increase in load as a result of the integration of thermal energy storage with the plant steam cycle. A study that investigates the feasibility of integrating thermal energy storage with thermal power plant steam cycles, considering different charging and discharging locations was also performed by (Li, D., Zhang, W., & Wang, 2018). This study demonstrated that thermal energy storage integration allows a faster response to load demand changes. The integration of a steam accumulator, known as Ruths storage, into a coal power plant to increase its flexibility was investigated by (Richter et al., 2019). It was found that the integrated energy storage is capable of allowing load change at a constant firing rate. In another study, storing the main steam sensible and latent heat during load ramping-down, in a molten salt and phase changing material, respectively, was proposed by (Wei et al., 2021). The stored heat was reused to heat the feed water and condensate water during the load ramping process, proving that the proposed operational concept improves the operational flexibility of a coal power plant and can make the unit operate at the lowest stable load. Furthermore, (Li & Wang, 2018) studied a strategy to integrate high-temperature thermal storage to the thermal power steam cycle of a power plant, identifying suitable charging and discharging locations in the steam cycle. The results showed the feasibility of extracting steam from the steam turbine to charge the thermal storage system and then discharge the stored heat to the power generation cycle, achieving a faster response to grid load demand changes. Finally, (Trojan et al., 2019) analyzed the improvement in the flexibility of a 200 MW_e unit by the integration of hot water storage tanks. A maximum increase in the unit power output resulted when hot water from the storage tanks was discharged to the boiler.

The studies conducted on thermal energy storage integration to fossil fuel power plants as an option to improve power plant flexibility has motivated research on thermal battery concepts capable of storing sensible heat in a thermally stable solid media, such as concrete, for easy integration with the thermal cycle of a fossil power plant. Additionally, solid media materials selected for this particular application should be cost-effective from a $/kWh point of view.

Several research groups have conducted investigations for the development of thermal batteries to store sensible heat in solid storage media to be used in different applications, such as solar power plants. Their results have shown the feasibility of storing sensible heat in solid storage media at relatively high temperatures. (Laing et al., 2006) reported development of two-storage system, composed of modules with two different storage materials and a tubular heat exchanger integrated into the storage material, with a capacity of 350 kWh_{th} each and a maximum operating temperature of 390°C. (Laing et al., 2009) reported test results of a 20 m^3 solid media storage module operated in the temperature range from 300°C and 400°C during 100 cycles. This project focused on the cost reduction of the heat exchanger and the high temperature concrete storage material. An approach for cost reduction using heat transfer structures with high thermal conductivity inside the concrete was presented by (Laing et al., 2012). In another research, (Tamme et al., 2004) analyzed solid media storage material properties and the geometry of the storage system as essential parameter for the economic optimization process of solid-state thermal batteries. (Salomoni et al., 2014) described the guidelines for designing a concrete storage module using a finite element method for the design of a scaled storage prototype. An experimental and numerical study of thermal energy storage using concrete, with upgraded thermo-mechanical properties, was conducted by (Giannuzzi et al., 2017). In this study, a new design of thermal cycling of storage elements for operation up to 400°C and based on the Joule effect heating was proposed. Additionally, an energy storage medium consisting of quartzite as a main component was presented by (Bergan & Greiner, 2014). This thermal energy system consists of steel pipes casted into concrete modules arranged in parallel and series which can be operated between 100 and 550°C. (Hoivik et al., 2019) also presented the performance of a two 500 kWh$_{th}$ thermal energy storage tested at the Masdar Institute Solar Platform at temperatures up to 380°C. This thermal energy storage system has a modular design consisting of steel pipe heat exchangers casted in concrete. The experimental results after 6,000 hours, confirmed the stability of material properties and showed no signs of degradation of the storage material.

This report describes experimental results of Lehigh University's new development on sensible thermal energy storage in concrete, which includes a novel approach regarding the way energy is transferred to/from the storage media during the charging and discharging process.

2. Concrete-Thermosiphon Thermal Battery Concept

Different than other thermal batteries where the heat transfer fluid (HTF) flows through pipes casted in large blocks of concrete or through thermal elements accommodated in series and parallel in a modular configuration, the novel thermal battery reported in this paper is configured with a dual action thermosiphon embedded in concrete engineered to operate up to 400°C with enhanced thermal and mechanical performance. This battery can operate with different types of heat transfer media, such as steam, flue gas or any other HTF, as well as heat transformed from electrical energy input if an easy access to low-cost renewable electric power is applicable.

The thermosiphon is a dual action device that can be used for charging and discharging purposes as shown in Figure 1. The dual action thermosiphon consists of a vacuumed pipe filled with an organic fluid . During the charging process as shown in Figure 1a), the bottom part of the thermosiphon (charging evaporator), which is below the concrete portion, is heated to evaporate the charged fluid that is inside the thermosiphon. Once evaporated, the fluid vapor raises, and it is condensed along the thermosiphon section that is inside the concrete (charging condenser). The condensed fluid returns to the evaporator along the thermosiphon pipe wall by gravity. In the charging condenser, the fluid's latent heat is transferred to the concrete. Because of the small temperature difference between the condenser and the evaporator, the effective thermal conductivity of the thermosiphon is higher than 10,000 W/m-K. As a result, an isothermal behavior is created along the length of the thermosiphon which allows a radial only heat transfer inside concrete.

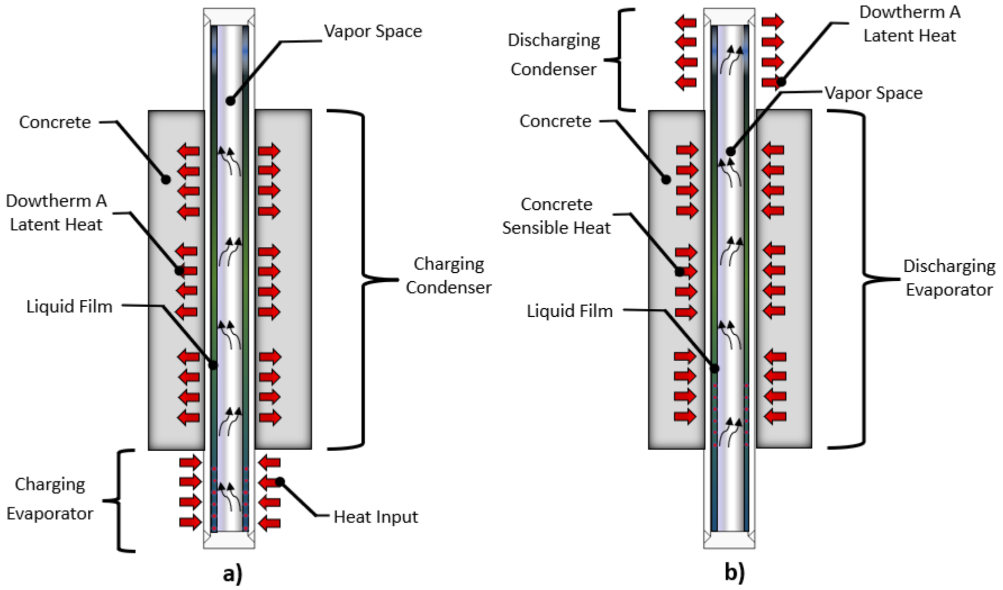

Figure 1. Dual action thermosiphon operation: a) charging and b) discharging

During the discharging process as shown in Figure 1b), the thermosiphon fluid is evaporated along the section of the thermosiphon embedded in the concrete (discharging evaporator), due to the high temperature of the concrete. The heat stored in the concrete during the charging process is now transferred to the fluid to allow its evaporation. The thermosiphon fluid vapor condenses at the top part of the thermosiphon outside the concrete portion (discharging condenser) and then returned to the bottom again by gravity. In the discharging condenser, the fluid latent heat is transferred to a heat transfer media.

3. Experimental Setup

Based on the concept described above, Lehigh University designed a 10 kWh_{th} TBC. This module was designed by embedding a dual action thermosiphon concentrically in a concrete cylinder enclosed in a steel jacket. The TBC was designed for operation with heated air as heat transfer media for both charging and discharging. The charging evaporator and the discharging condenser consist of two separate steel plenums designed for optimized flow field and heat transfer with thermosiphon finned sections inside of them, transferring heat by convection during the charging and discharging processes. A schematic of the Lehigh 10 kWh_{th} TBC is shown in Figure 2.

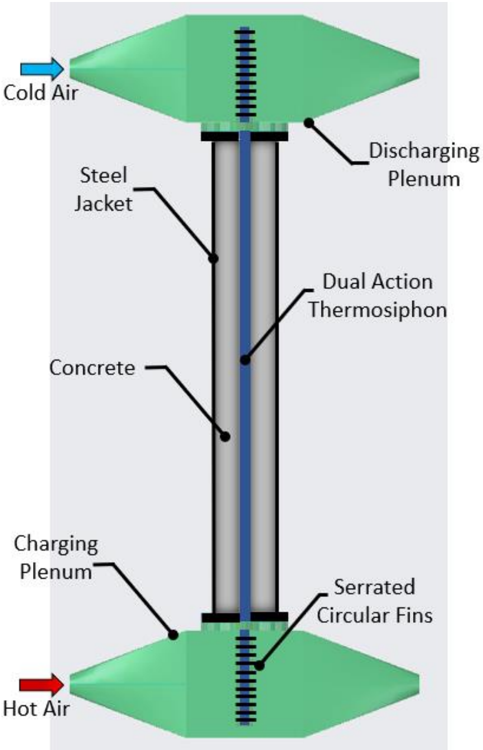

Figure 2. Lehigh University 10-kWh_{th} TBC schematic

The experimental test rig consists of a 10.5 ft long thermosiphon concentrically embedded in a 14 in diameter, 7 ft long, concrete cylinder. The concrete cylinder was casted inside a 14 in schedule 40 steel pipe. The average concrete specific heat (C_p), density (ρ) and thermal conductivity (k) in the operation temperature range 300-400°C are 1.1 kJ/kg K, 2,300 kg/m^3 and 1.88 W/m-K, respectively. The thermosiphon used in this test has a 1.5 in inside diameter (ID), a 1.9 in outside diameter (OD), a 10.5 ft length and is made of a low carbon pipe 25% filled in volume with the thermosiphon thermal fluid. Low carbon steel serrated circular fins with 1 in height were fitted at both ends of the thermosiphon to increase the heat transfer area. The finned section length at the bottom and top of the thermosiphon is 18 in and 21 in, respectively. The TBC was insulated with a 5 in mineral wool layer. The insulation was covered with aluminum foil to reduce radiation heat losses. Figure 3a shows a photograph of the thermosiphon embedded in the concrete cylinder and the serrated circular fins on one end.

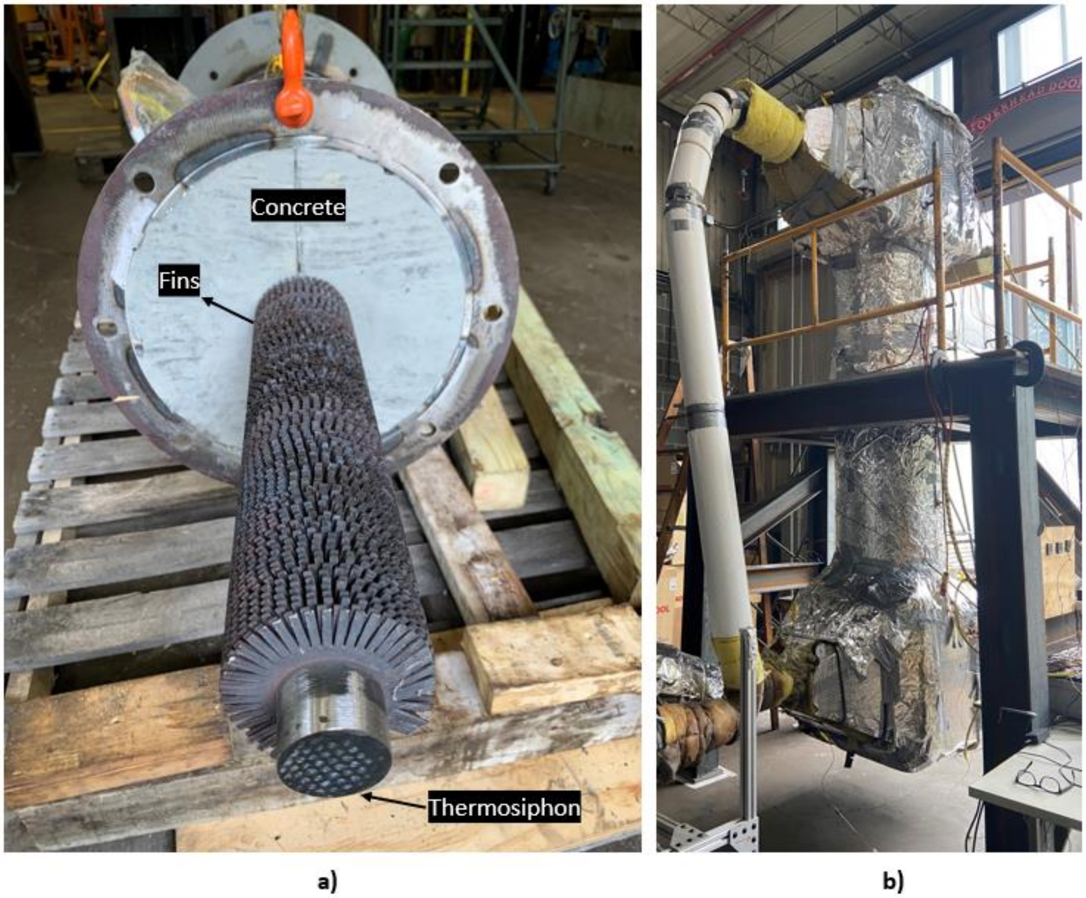

Figure 3. a) Finned thermosiphon embedded in concrete; b) Insulated concrete cylinder and plenums

Two 75 kW electrical heaters were used as energy supply to heat the air used as heat transfer media for the charging and discharging processes. The air temperature used for charging and discharging was 433 °C and 185°C, respectively. Two 3/8 in thick low carbon steel plenums were fabricated and connected with the top and bottom steel jacket flange of the concrete cylinder. Each plenum consists of two adapting parts from a 3 in diameter pipe to a 20 in by 18 in by 24 in rectangular box. Figure 3b shows a picture of the system with plenums and insulation layer installed in place.

Twenty-five type K thermocouples, with an accuracy of ± 0.75%, were placed longitudinally through the thermosiphon and radially inside the concrete. A Campbell-Scientific CR9000X data logger was used to record the temperature history during the testing. The thermocouples were placed inside concrete at five equidistant levels with a 21 in spacing staring from the bottom surface of concrete. For each vertical level, five equidistant thermocouples were placed along the radial direction with a 1.5 in spacing starting from the thermosiphon surface. Figure 4 illustrates the position of the thermocouples in the experimental setup. Additionally, thermocouples were placed on the external surface of the insulation layer, and at the inlet and outlet of two plenums. The ambient temperature was also recorded during the testing. The air flow rate was measured at 25°C using an electronic flowmeter with an accuracy of ± 5%.

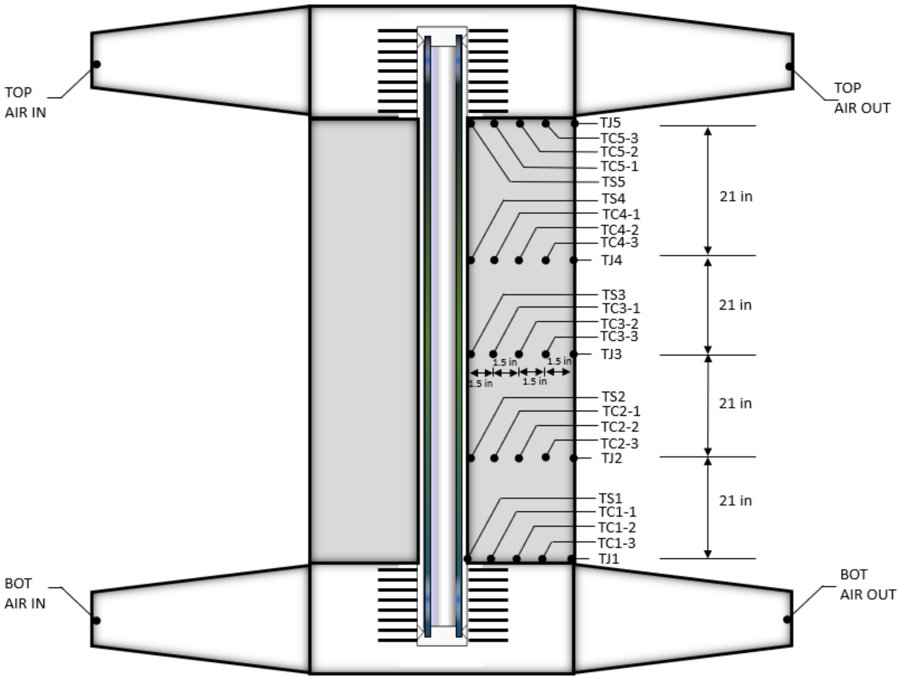

Figure 4. Thermocouples position in experimental setup

The piping and instrumentation diagram (P&ID) of the experimental setup is shown in Figure 5. At the beginning of the charging process, the valves located at the inlet and outlet of the charging plenum (Valves Charge 1, 2 and 3) are open to allow the hot air to flow through the charging plenum while the valves located at the inlet and outlet of the discharging plenum (Valves discharge 1, 2 and 3) are closed to prevent any air flowing through the discharge plenum.

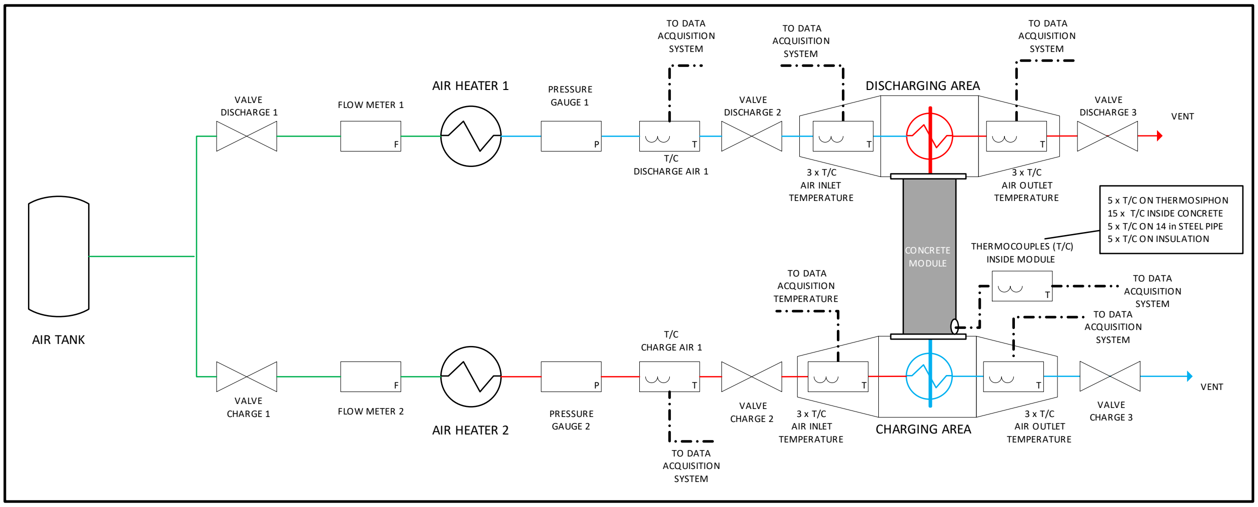

Figure 5. Experimental setup P&ID

After the charging process and holding periods are concluded, the valves located at the inlet and outlet of the charging plenum are closed to stop air flowing through it while the valves located at the inlet and outlet of the discharging plenum are open to allow the colder air to flow through this plenum.

4. Experimental Results

During the charging process, air at 433°C was circulated through the insulated plenum located at the bottom of the concrete module. An air mass flow rate of 0.16 kg/s was used for all the tests. As shown in Figure 6 from a charging test, 10 kWh thermal energy storage objective is achieved after 6.3 hours, including energy stored in concrete, thermosiphon pipe and steel jacket. The specific capacity of the Lehigh University TBC (including the storage material, the dual action thermosiphon and the steel jacket) is 47.2 kWh/m^3.

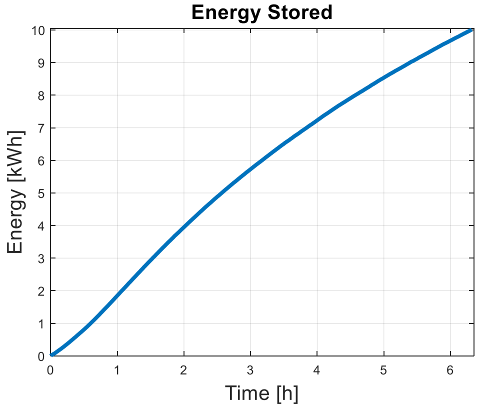

Figure 6. Energy stored in TBC during charging

Figure 7 shows the corresponding temperature of the air at inlet and outlet of the charging plenum and thermosiphon-concrete interface during the charging process. A temperature difference of 30°C between the air inlet and outlet temperatures is shown in Figure 7. This demonstrates that an effective heat transfer between the air and the fins occurs inside the plenum. The maximum temperature difference along the length of thermosiphon is 8°C which is observed between the top and bottom of the thermosiphon. This temperature difference along the thermosiphon confirms the isothermal behavior of the thermosiphon is well maintained during the charging testing. Furthermore, this temperature distribution along the thermosiphon height allows to consider the heat transfer in the concrete only in radial direction. During the testing, it is found that the average thermosiphon temperature first rapidly increased from 200°C to 335°C in an hour and then slowly increased from 335°C to 360°C in the next five hours due to the limitation of the air input temperature constantly at 433°C.

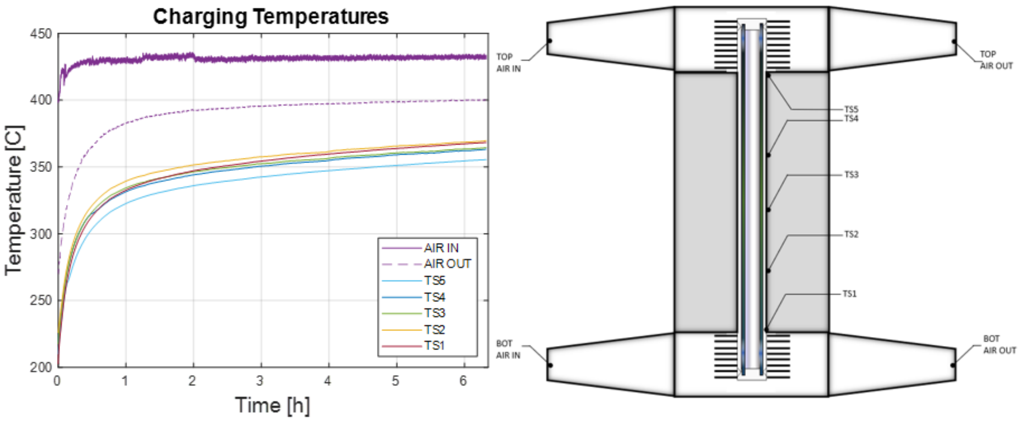

Figure 7. Temperatures of air, thermosiphon and concrete during charging process

Figure 8 shows concrete temperature contours at the beginning and the end of the charging process. As expected, the temperature distribution along the vicinity of the thermosiphon is constant while the distribution propagates into the concrete mainly in the radial direction. The temperature propagation in relation to the bottom and top of the concrete is due to the use of only one thermosiphon to heat the concrete mass needed to store 10 kWh_{th}.

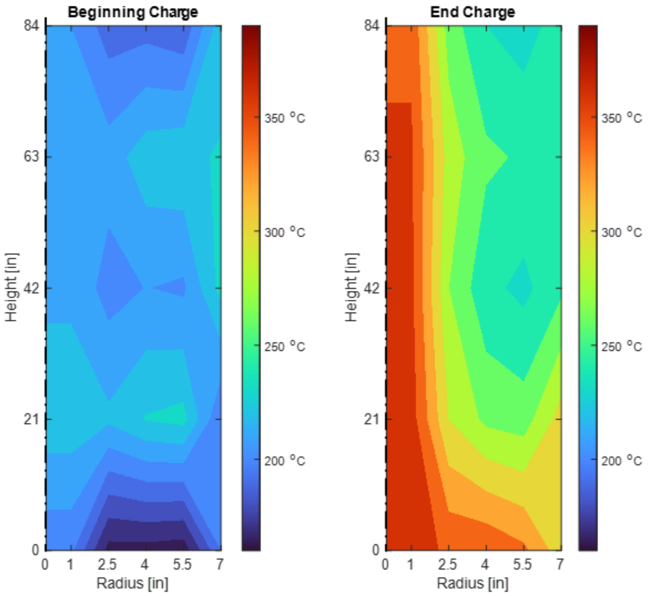

Figure 8. Concrete temperature contours at the beginning and end of the charging process

In the next stage of this research, several thermosiphons in an optimized distribution will be embedded to reach uniform radial and axial temperatures in the concrete. The beginning of the 100 kWh_{th} TBC construction and assemble is shown in Figure 9.

Figure 9. Beginning of 100 kWh_{th} construction and assemble

During the discharging process, air at 185°C was circulated through the discharging plenum at the top of the concrete module. Four tests were performed using four different air mass flow rates: 0.16, 0.11, 0.011, and 0.008 kg/s. After a duration of 3.8 hours, the thermal energy discharged from the module was 5.9, 5.6, 4.9 and 4.2 kWh_{th}, respectively. The history of released energy amount during the discharging testing is shown in Figure 10.

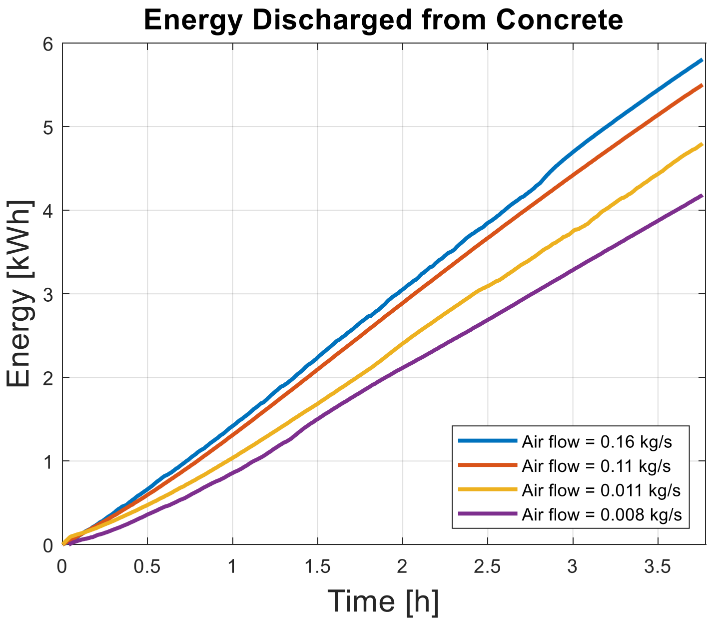

Figure 10. Energy discharged during discharge tests

The discharging initial conditions, for the four discharge tests, were the same as well as the tests duration. The energy transferred to the air was 4.3, 4, 1.7 and 1.3 kWh_{th} for each one of the air mass flow rates. The results for the four discharging tests are presented in Table 1.

Table 1. Discharge tests results

Test	Test time [h]	Air mass flow [kg/s]	Energy from Concrete [kWh_{th}]	Energy to Air [kWh_{th}]
1	3.8	0.16	5.8	4.3
2	3.8	0.11	5.5	4.0
3	3.8	0.011	4.8	1.7
4	3.8	0.008	4.2	1.3

Figure 11 shows the air and thermosiphon-concrete interface temperatures for the discharging process test performed using an air mass flow rate of 0.008 kg/s. The air temperature difference between the inlet and outlet of the plenum decreases slightly with time and it is approximately 30°C at the end of the discharge test. This reduction is expected as the thermosiphon temperature decreased with time. The air temperature difference, between the plenum inlet and outlet, demonstrates that an effective heat transfer between the air and the fins occurs inside the plenum.

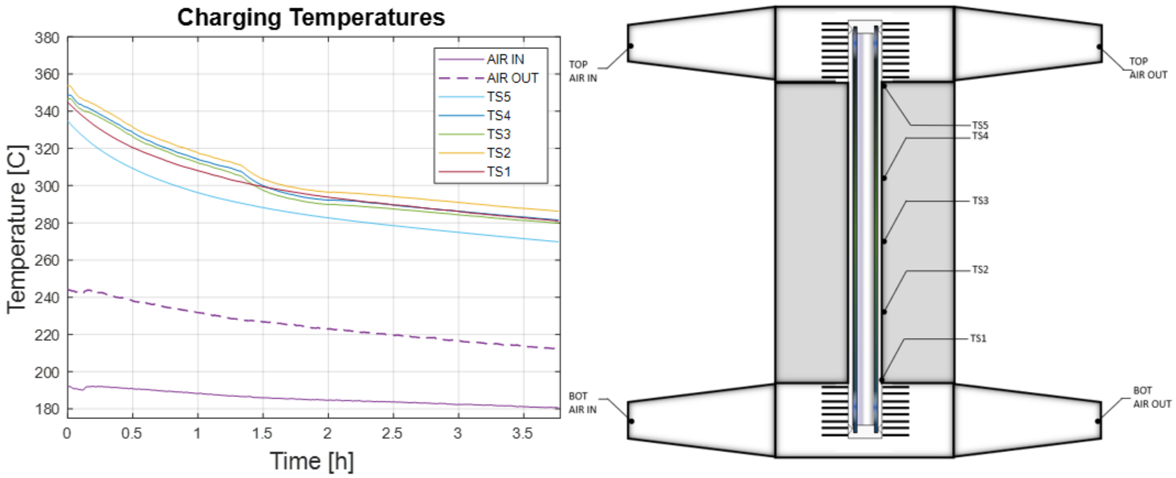

Figure 11. Air, thermosiphon and concrete temperatures of 0.008 kg/s discharging test

Figure 12 shows the concrete cylinder temperature contours at the beginning and the end of the discharging process when an air mass flow rate of 0.008 kg/s was used.

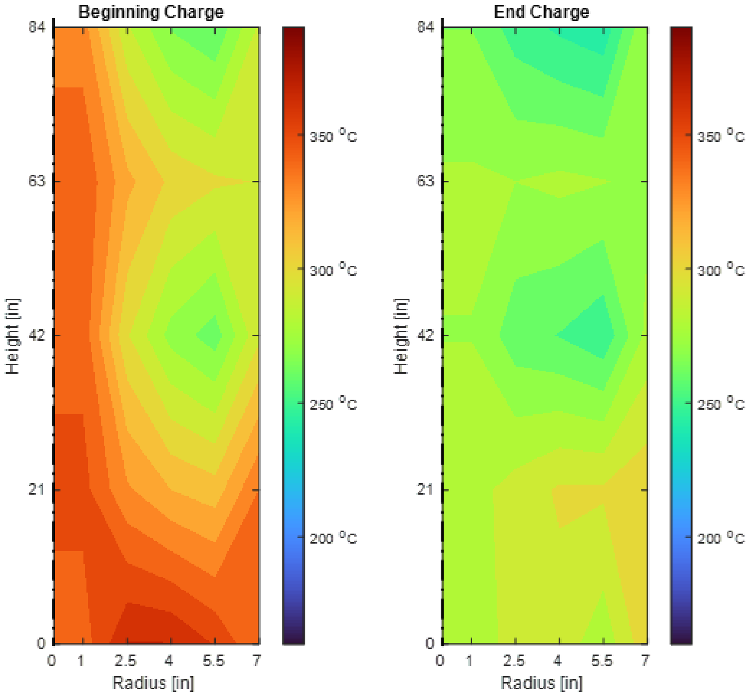

Figure 12. Concrete temperature contours at the beginning and end of 0.008 kg/s discharge test

5. Conclusions

A dual action thermosiphon embedded inside concrete with optimized thermal and mechanical behavior concept was demonstrated at Lehigh University as a feasible way to storage thermal energy for fuel fired power plant flexibilization. The concrete-thermosiphon thermal battery demonstrated to have a rapid heat transfer response to/from the storage media. Testing performed at chosen air mass flow rate showed the proposed thermal battery system has the ability to be charged and discharged in the temperature range between 300 and 400°C. A small temperature difference along the thermosiphon length during both charging and discharging testing is found demonstrating the thermosiphon is able to maintain an isothermal behavior during the operation of the system. It is confirmed based on the measurements that the heat transfer throughout concrete is mainly on the radial direction, which can be used as a practical assumption for analytical studies. An air temperature difference between the plenum inlet and outlet, during the charging and discharging processes, indicates that an effective heat transfer between the air and the fins occurs inside the plenums.

6. Acknowledgments

"This material is based upon work supported by the Department of Energy Award Number DE-FE0031755".

Disclaimer: "This report was prepared as an account of work sponsored by an agency of the United States Government. Neither the United States Government nor any agency thereof, nor any of their employees, makes any warranty, express or implied, or assumes any legal liability or responsibility for the accuracy, completeness, or usefulness of any information, apparatus, product, or process disclosed, or represents that its use would not infringe privately owned rights. Reference herein to any specific commercial product, process, or service by trade name, trademark, manufacturer, or otherwise does not necessarily constitute or imply its endorsement, recommendation, or favoring by the United States Government or any agency thereof. The views and opinions of authors expressed herein do not necessarily state or reflect those of the United States Government or any agency thereof."

7. References

Bergan, P. G., & Greiner, C. J. (2014). A New Type of Large Scale Thermal Energy Storage. *Energy Procedia*, *58*(1876), 152–159. https://doi.org/10.1016/j.egypro.2014.10.422

Cao, R., Lu, Y., Yu, D., Guo, Y., Bao, W., Zhang, Z., & Yang, C. (2020). A novel approach to improving load flexibility of coal-fired power plant by integrating high temperature thermal energy storage through additional thermodynamic cycle. *Applied Thermal Engineering*, *173*(August 2019), 115225. https://doi.org/10.1016/j.applthermaleng.2020.115225

Giannuzzi, G. M., Liberatore, R., Mele, D., Mazzucco, G., Xotta, G., Salomoni, V. A., Majorana, C. E., & Di Maggio, R. (2017). Experimental campaign and numerical analyses of thermal storage concrete modules. *Solar Energy*, *157*(January 2016), 596–602. https://doi.org/10.1016/j.solener.2017.08.041

Hoivik, N., Greiner, C., Barragan, J., Iniesta, A. C., Skeie, G., Bergan, P., Blanco-Rodriguez, P., & Calvet, N. (2019). Long-term performance results of concrete-based modular thermal energy storage system. *Journal of Energy Storage*, *24*(April), 100735. https://doi.org/10.1016/j.est.2019.04.009

Laing, D., Bahl, C., Bauer, T., Fiss, M., Breidenbach, N., & Hempel, M. (2012). High-temperature solid-media thermal energy storage for solar thermal power plants. *Proceedings of the IEEE*, *100*(2), 516–524. https://doi.org/10.1109/JPROC.2011.2154290

Laing, D., Lehmann, D., Fi, M., & Bahl, C. (2009). Test results of concrete thermal energy storage for parabolic trough power plants. *Journal of Solar Energy Engineering, Transactions of the ASME*, *131*(4), 0410071–0410076. https://doi.org/10.1115/1.3197844

Laing, D., Steinmann, W. D., Tamme, R., & Richter, C. (2006). Solid media thermal storage for parabolic trough power plants. *Solar Energy*, *80*(10), 1283–1289.

https://doi.org/10.1016/j.solener.2006.06.003

Li, D., Zhang, W., & Wang, J. (2018). Flexible Operation of Supercritical Power Plant via Integration of Thermal Energy Storage. In *In (Ed.), Power Plants in the Industry. IntechOpen*. https://doi.org/https://doi.org/10.5772/intechopen.79735

Li, D., & Wang, J. (2018). Study of supercritical power plant integration with high temperature thermal energy storage for flexible operation. *Journal of Energy Storage*, *20*(September), 140–152. https://doi.org/10.1016/j.est.2018.09.008

Richter, M., Möllenbruck, F., Starinsk, A., Oeljeklaus, G., & Görner, K. (2015). Flexibilization of Coal-fired Power Plants by Dynamic Simulation. *Proceedings of the 11th International Modelica Conference, Versailles, France, September 21-23, 2015*, *118*(September), 715–723. https://doi.org/10.3384/ecp15118715

Richter, M., Oeljeklaus, G., & Görner, K. (2019). Improving the load flexibility of coal-fired power plants by the integration of a thermal energy storage. *Applied Energy*, *236*(September 2018), 607–621. https://doi.org/10.1016/j.apenergy.2018.11.099

Salomoni, V. A., Majorana, C. E., Giannuzzi, G. M., Miliozzi, A., Di Maggio, R., Girardi, F., Mele, D., & Lucentini, M. (2014). Thermal storage of sensible heat using concrete modules in solar power plants. *Solar Energy*, *103*, 303–315. https://doi.org/10.1016/j.solener.2014.02.022

Tamme, R., Laing, D., & Steinmann, W. D. (2004). Advanced thermal energy storage technology for parabolic trough. *Journal of Solar Energy Engineering, Transactions of the ASME*, *126*(2), 794–800. https://doi.org/10.1115/1.1687404

Trojan, M., Taler, D., Dzierwa, P., Taler, J., Kaczmarski, K., & Wrona, J. (2019). The use of pressure hot water storage tanks to improve the energy flexibility of the steam power unit. *Energy*, *173*, 926–936. https://doi.org/10.1016/j.energy.2019.02.059

Wei, H., Lu, Y., Yang, Y., Zhang, C., He, C., Wu, Y., Li, W., & Zhao, D. (2021). Research on influence of steam extraction parameters and operation load on operational flexibility of coal-fired power plant. *Applied Thermal Engineering*, *195*(May), 117226. https://doi.org/10.1016/j.applthermaleng.2021.117226